

Received 22 January 2020

Accepted 16 March 2020

Edited by C. Massera, Università di Parma, Italy

Keywords: crystal structure; anti-TB activity drug; intermolecular interactions; Hirshfeld surface analysis; fingerprint plot.

CCDC reference: 1865697

Supporting information: this article has supporting information at journals.iucr.org/e

Structural investigation of methyl 3-(4-fluoro-benzoyl)-7-methyl-2-phenylindolizine-1-carboxylate, an inhibitory drug towards *Mycobacterium tuberculosis*

Avantika Hasija,^a Subhrajyoti Bhandary,^a Katharigatta N. Venugopala,^{b,c} Sandeep Chandrashekharappa^d and Deepak Chopra^{a*}

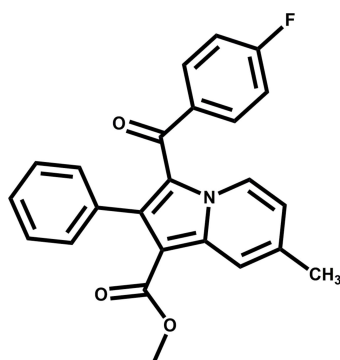
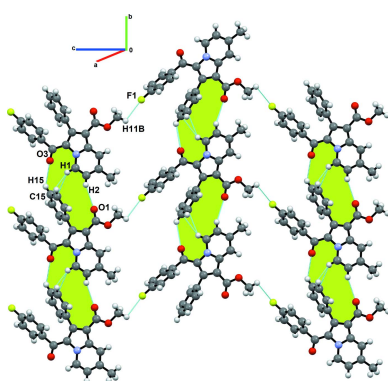
^aDepartment of Chemistry, Indian Institute of Science Education and Research Bhopal, Bhauri, Bhopal 462066, India,

^bDepartment of Pharmaceutical Sciences, College of Clinical Pharmacy, King Faisal University, Al-Ahsa 31982, Kingdom of Saudi Arabia, ^cDepartment of Biotechnology and Food Technology, Durban University of Technology, Durban 4001, South Africa, and ^dInstitute for Stem Cell Biology and Regenerative Medicine, NCBS, TIFR, GKVK, Bellary Road, Bangalore 560 065, India. *Correspondence e-mail: dchopra@iiserb.ac.in

The title compound, $C_{24}H_{18}FNO_3$, crystallizes in the monoclinic centrosymmetric space group $P2_1/n$ and its molecular conformation is stabilized via $C-H\cdots O$ intramolecular interactions. The supramolecular network mainly comprises $C-H\cdots O$, $C-H\cdots F$ and $C-H\cdots \pi$ interactions, which contribute towards the formation of the crystal structure. The different intermolecular interactions have been further analysed via Hirshfeld surface analysis and fingerprint plots.

1. Chemical context

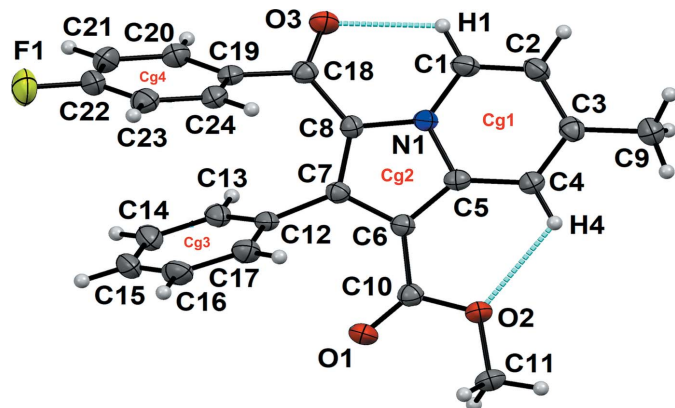
Indolizine represents an interesting heterocyclic scaffold in which the nitrogen atom belongs to both of the fused six- and five-membered rings. It is a well-known pharmacophore endowed with various promising pharmacological properties. For instance, indolizines have been found to exhibit analgesic (Vaught *et al.*, 1990), anticancer (Butler, 2008; Sandeep *et al.*, 2016*a,b*), antidiabetic (Mederski *et al.*, 2012), antihistaminic (Cingolani *et al.*, 1990), anti-microbial (Hazra *et al.*, 2011) and antiviral (Mishra & Tiwari, 2011) activity. It has also been found to act as cyclo-oxygenase (COX-2) inhibitor (Chandrashekharappa *et al.*, 2018*b*) and to have larvicidal activity against *Anopheles arabiensis* (Chandrashekharappa *et al.*, 2018*a*).



The title compound, comprising a substituted indolizine unit, displays a modest activity against susceptible H37Rv strains of *Mycobacterium tuberculosis* (Venugopala *et al.*, 2019). Besides the tremendous scope of the pharmacological studies on indolizine-based compounds, the substitution of



OPEN ACCESS

**Figure 1**

Ellipsoid plot of the title compound drawn with 50% probability ellipsoids. Dotted lines indicate intramolecular C–H···O interactions. Cg_1 , Cg_3 and Cg_4 represent the centroids of the six-membered rings $N1/C1-C9$, $C1-C5$, $C12-C17$ and $C18/O3/C19-C24/F1$, respectively, while Cg_2 represents the five-membered ring $N1/C5-C8$.

fluorine on the benzoyl ring, the presence of flexible moieties and of competitive hydrogen-bond acceptors (namely, oxygen O2 in the ester group at C6 and O3 in the carbonyl group at C8) make the structural study of the title compound of extreme relevance. In addition, it is of importance to observe the cooperative interplay of weak interactions that contribute towards the consolidation of the crystal lattice. In the present paper, we report the molecular and crystal structure of the title compound, highlighting its molecular conformation and analysing the different intermolecular interactions *via* Hirshfeld surface analysis and fingerprint plots.

2. Structural commentary

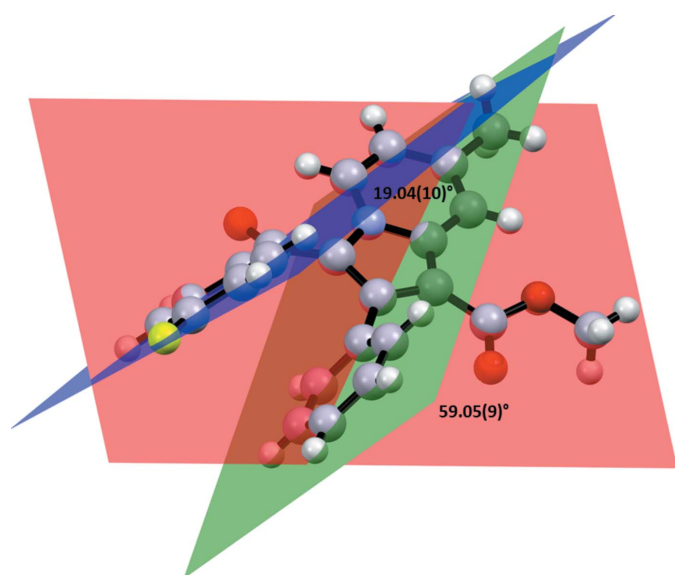
The title compound crystallizes in the centrosymmetric monoclinic $P2_1/n$ space group. The molecular structure

Table 1
Hydrogen-bond geometry (\AA , $^\circ$).

$D-\text{H}\cdots A$	$D-\text{H}$	$\text{H}\cdots A$	$D\cdots A$	$D-\text{H}\cdots A$
$C1-\text{H}1\cdots O3$	0.95	2.26	2.853 (3)	120
$C4-\text{H}4\cdots O2$	0.95	2.38	2.927 (2)	116
$C21-\text{H}21\cdots O3^i$	0.95	2.54	3.399 (3)	149
$C2-\text{H}2\cdots O1^{ii}$	0.95	2.63	3.531 (4)	157
$C15-\text{H}15\cdots O3^{iii}$	0.95	2.76	3.519 (4)	137
$C1-\text{H}1\cdots C15^{ii}$	0.95	2.74	3.6064 (3)	152
$C11-\text{H}11A\cdots C5^{iv}$	0.98	2.74	3.4906 (1)	133
$C11-\text{H}11B\cdots F1^v$	0.98	2.67	3.0585 (3)	104
$C23-\text{H}23\cdots O3^{vi}$	0.95	2.67	3.4875 (3)	143

Symmetry codes: (i) $-x + \frac{3}{2}, y + \frac{1}{2}, -z + \frac{1}{2}$; (ii) $x, y - 1, z$; (iii) $x, y + 1, z$; (iv) $-x, -y + 1, -z$; (v) $x - \frac{1}{2}, -y + \frac{3}{2}, z - \frac{1}{2}$; (vi) $-x + \frac{1}{2}, y + \frac{1}{2}, -z + \frac{1}{2}$.

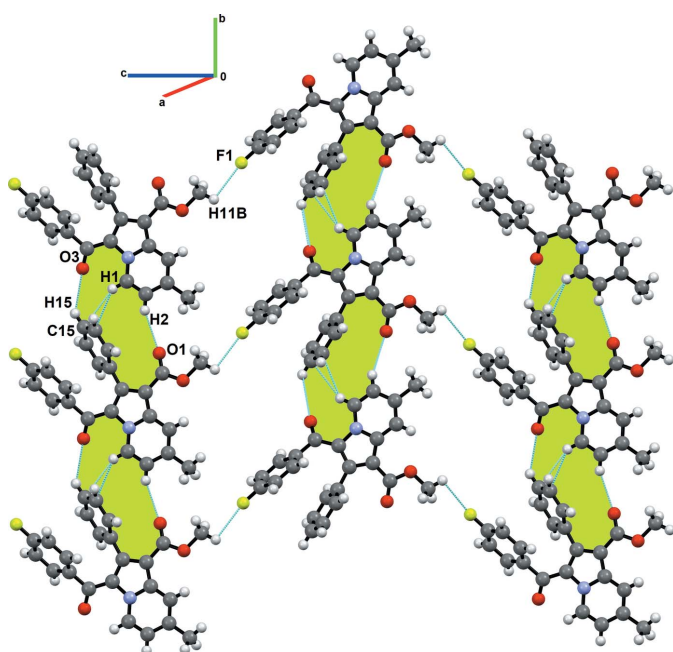
comprises one methylindolizine heterocyclic moiety ($N1/C1-C9$) consisting of fused six- and five-membered rings ($N1/C1-C5$, centroid Cg_1 and $N1/C5-C8$, centroid Cg_2). The heterocycle is substituted at the carbon atoms C6, C7 and C8 with a methoxy carbonyl group, a phenyl ring ($C12-C17$, centroid Cg_3), and a fluorobenzoyl ring [$C18/O3/C19-C24/F1$, centroid Cg_4], respectively (Fig. 1). The molecular structure possesses three conformational degrees of freedom due to the free rotation with respect to the $C6-C10$, $C7-C12$, and $C8-C18$ single bonds. The molecular conformation is stabilized by the presence of intramolecular $C1-\text{H}1\cdots O3$ [$C1\cdots O3 = 2.853$ (3) \AA] and $C4-\text{H}4\cdots O2$ [$C4\cdots O2 = 2.927$ (2) \AA] interactions (Table 1) and by $\pi-\pi$ stacking [$Cg_3\cdots Cg_4 = 3.5084$ (13) \AA]. The dihedral angle between the mean plane through ring Cg_3 (coloured in green in Fig. 2) and the mean plane of the indolizine skeleton (coloured in red) is 59.05 (9) $^\circ$, while the dihedral angle between the mean plane through the phenyl ring and that through the fluorobenzoyl ring (coloured in blue) is as small as 19.04 (10) $^\circ$, showing the nearly parallel position of the rings. The torsion angles $N1-C8-C18-C19$ and $C8-C18-C19-C24$ are -161.74 (19) and 46.2 (3) $^\circ$, respectively.

**Figure 2**

Dihedral angles between the mean plane passing through the $C12-C17$ ring (green) and the $C18/O3/C19-C24/F1$ ring (blue) and through the indolizine skeleton (red).

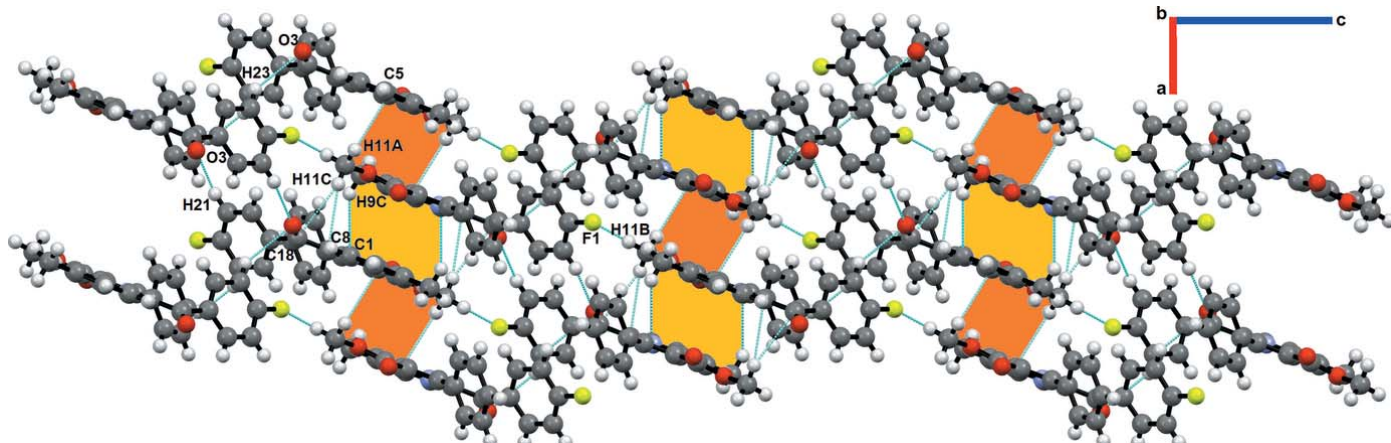
3. Supramolecular features

The list of all intra- and intermolecular interactions along with their geometrical parameters have been reported in Table 1. The interactions included for investigation are based on the distance criteria of $\text{vdW} + 0.4$ \AA (Dance, 2003). In the crystal, the molecules are primarily assembled through concomitant $C21-\text{H}21\cdots O1^{ii}/O3^{iii}$ interactions [$C21\cdots O1^{ii} = 3.531$ (4) \AA , 157° ; $C15\cdots O3^{iii} = 3.519$ (4) \AA , 137° ; symmetry codes: (ii) $x, y - 1, z$; (iii) $x, y + 1, z$] and $C1-\text{H}1\cdots \pi(C15)^{ii}$ [$C1\cdots C15 = 3.6064$ (3) \AA , 152°], forming ribbons along the [010] direction, as shown by the green shading in Fig. 3. Two adjacent ribbons are connected to each other *via* $C11-\text{H}11B\cdots F1^v$ [$C11\cdots F1 = 3.0585$ (3) \AA , 104° ; symmetry code: (v) $x - \frac{1}{2}, -y + \frac{3}{2}, z - \frac{1}{2}$] (Fig. 3) and $C21-\text{H}21\cdots O3^i$ [$C21\cdots O3 = 3.399$ (3) \AA , 149° ; symmetry code: (i) $-x + \frac{3}{2}, y + \frac{1}{2}, -z + \frac{1}{2}$] (Fig. 4) interactions in a zigzag fashion along [001], resulting in the formation of a molecular sheet parallel to the ac plane. Analogous C–H···F interactions have been investigated, showing that where the angularity is in the range 90 to

**Figure 3**

Crystal packing of title compound showing the formation of molecular sheets parallel to the bc plane *via* $\text{C}-\text{H}\cdots\text{O}$, $\text{C}-\text{H}\cdots\pi$ and $\text{C}-\text{H}\cdots\text{F}$ interactions.

140° , the σ -hole on fluorine is directed towards the electron density of the $\text{C}-\text{H}$ bond (Hathwar *et al.*, 2020), underlining the importance of interactions with low angularity. The molecular sheets are closely stacked along the a -axis direction *via* weak interactions such as $\text{C9}-\text{H9C}\cdots\pi(\text{C1})$ [$\text{C9}\cdots\text{C1}^{\text{vii}} = 3.7431(5)$ Å; symmetry code: (vii) $-x + 1, -y, -z$], $\text{C11}-\text{H11A}\cdots\pi(\text{C5})$ [$\text{C11}\cdots\text{C5}^{\text{iv}} = 3.4906(4)$ Å; symmetry code: (iv) $-x, -y + 1, -z$], $\text{C11}-\text{H11C}\cdots\pi(\text{C8})$ [$\text{C11}\cdots\text{C8}^{\text{viii}} = 3.6590(5)$ Å; symmetry code: (viii) $-x + 1, -y + 1, -z$] (Fig. 4), giving rise to a layered supramolecular structure. From this analysis, it can be stated that the formation of the crystal structure is mainly governed by several $\text{C}-\text{H}\cdots\text{O}$ and $\text{C}-\text{H}\cdots\pi$ interactions, while the $\text{C}-\text{H}\cdots\text{F}$ interactions play a secondary but supporting role in its overall consolidation.

**Figure 4**

Stacking of molecular sheets along the a -axis direction, primarily *via* $\text{C}-\text{H}\cdots\pi$ and $\text{C}-\text{H}\cdots\text{F}$ interactions, resulting in a layered supramolecular architecture.

4. Database survey

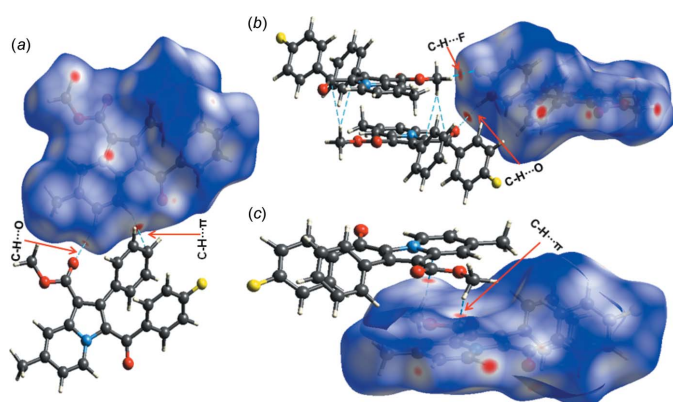
A search for the 2-phenylindolizine skeleton in the CSD (version 5.40, update of August 2019; Groom *et al.*, 2016) was carried out. Out of the 39 hits for unsubstituted phenyl rings attached to indolizine, the majority of entries gave reports of varied synthetic procedures and methodologies to obtain these compounds, underlining their importance. The near-infrared emissive properties of KIVLIN, KIVLOT, KIVLUZ (Gayton *et al.*, 2019) and KENFAN (McNamara *et al.*, 2017) have also been reported.

Structural details of compounds such as CAJTAI (Aslanov *et al.*, 1983), EMUTOV (Liu, *et al.*, 2003), FEDQAH (Liu, *et al.*, 2005), GIYLOP (Sonnenschein & Schneider, 1997), ODEFIN (Qian *et al.*, 2006), PNOIZA, PNOIZB, PNOIZE, PNOIZF (Tafeenkov & Aslanov, 1980), ROLKIM (Tafeenkov & Au, 1996) and TIGXOX (Liu, *et al.*, 2007) have also been deposited. Almost all of these molecules are substituted at the C8 position with electron-withdrawing substituents such as $-\text{COMe}$, $-\text{CH}_2\text{CN}$, $-\text{CN}$, $-\text{N}=\text{O}$, $-\text{CH}=\text{C}(\text{Ph})(\text{CN})$, etc.

In particular, the papers reporting TIGXOX (Liu *et al.*, 2007), FEDQAH (Liu *et al.*, 2005) and ODEFIN (Qian *et al.*, 2006) discuss the structural features of molecules comprising the 2-phenyl indolizine skeleton, showing high fluorescent efficiency. In these reports, the respective dihedral angles between the mean plane of the indolizine skeleton and the plane of the phenyl ring are *ca* 53, 39 and 49 and 45° , comparable to that reported in the title compound.

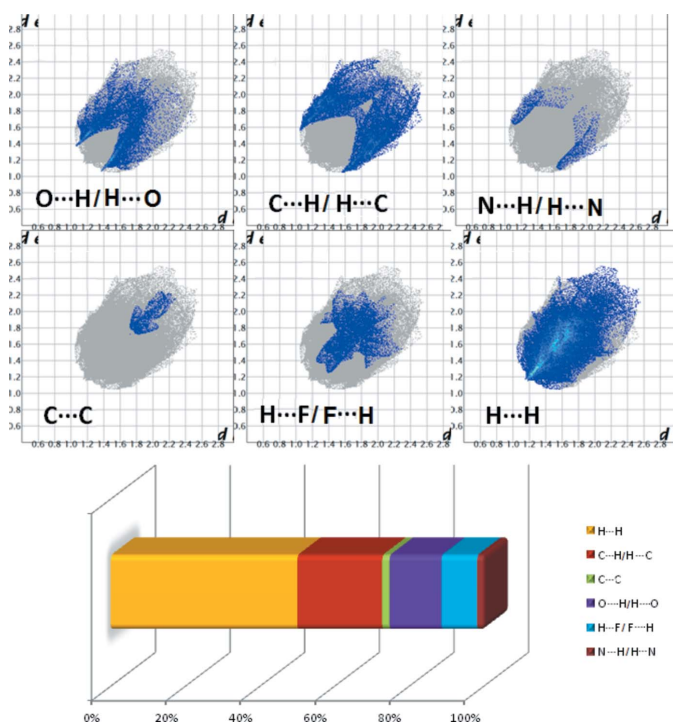
5. Hirshfeld surface analysis and fingerprint plots

The significance of the cumulative effect of the interactions involved in the crystal structure can be visualized qualitatively through Hirshfeld surface analysis (Spackman *et al.*, 2009). The Hirshfeld surfaces and the two-dimensional fingerprint plots were calculated using *CrystalExplorer* (Version 17.5; Wolff *et al.*, 2012) and are shown in Figs. 5 and 6, respectively. The red spots on the HS surface illustrate the presence of

**Figure 5**

The Hirshfeld surface of title compound mapped over d_{norm} . Dashed lines indicate hydrogen bonds.

supramolecular interactions such as C—H···O, C—H··· π and C—H···F whereas the blue regions indicate the lack of contact distances shorter than the sum of the van der Waals radii. The fingerprint plots represent the individual contributions of the different interactions. Fig. 6 shows that the major contribution comes from H···H (47.1%), O···H/H···O (13.1%), C···H/H···C (21.4%), H···F/F···H (9.0%), C···C (1.9%) and N···H/H···N (1.7%) contacts. The relatively high percentage of C···H/H···C contacts indicates how the contribution of all of the C—H··· π interactions plays an important role in consolidating the crystal packing.

**Figure 6**

The fingerprint plots of the title compound showing the different contributions deriving from the O···H/H···O, N···H/H···N, C···H···C, H···F/F···H, C···C and H···H contacts.

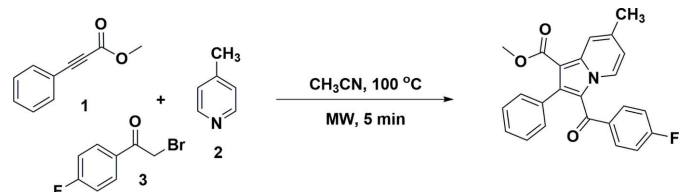
Table 2
Experimental details.

Crystal data	
Chemical formula	C ₂₄ H ₁₈ FNO ₃
M _r	387.39
Crystal system, space group	Monoclinic, P2 ₁ /n
Temperature (K)	173
a, b, c (Å)	7.3246 (11), 9.8460 (13), 25.837 (4)
β (°)	93.318 (3)
V (Å ³)	1860.2 (5)
Z	4
Radiation type	Mo K α
μ (mm ⁻¹)	0.10
Crystal size (mm)	0.32 × 0.18 × 0.04
Data collection	
Diffractometer	Bruker Kappa Duo APEXII
Absorption correction	Multi-scan (SADABS; Bruker, 2008)
T_{\min} , T_{\max}	0.855, 1.000
No. of measured, independent and observed [$I > 2\sigma(I)$] reflections	27523, 4296, 2641
R_{int}	0.090
(sin θ/λ) _{max} (Å ⁻¹)	0.652
Refinement	
$R[F^2 > 2\sigma(F^2)]$, $wR(F^2)$, S	0.050, 0.131, 1.00
No. of reflections	4296
No. of parameters	265
H-atom treatment	H-atom parameters constrained
$\Delta\rho_{\text{max}}$, $\Delta\rho_{\text{min}}$ (e Å ⁻³)	0.29, -0.30

Computer programs: APEX2 (Bruker, 2012), SAINT (Bruker, 2008), SHELXS97 (Sheldrick, 2008), X-SEED (Barbour, 2001), Mercury (Macrae *et al.*, 2020), SHELXL2014 (Sheldrick, 2015) and PLATON (Spek, 2020).

6. Synthesis and crystallization

All chemicals were obtained from Sigma–Aldrich and used without further purification. A mixture of methyl 3-phenylpropiolate (**1**) (160 mg, 1 mmol), 4-methylpyridine (**2**) (93 mg, 1 mmol), 2-bromo-1-(4-fluorophenyl)ethan-1-one (**3**) (217 mg, 1 mmol), and triethylamine (0.101 mg, 1 mmol) in 4.5 mL of acetonitrile were added to a 10 mL microwave tube under a nitrogen atmosphere (Fig. 7). A microwave initiator was used to irradiate the reaction mixture at 373 K for about 5 min. The reaction was monitored *via* TLC. The solvent was then removed under reduced pressure, the crude residue was diluted with water and the aqueous layer was extracted twice with ethyl acetate, and the combined organic solvent was washed with a brine solution. The organic layer was removed under reduced pressure and the remaining residue was subjected to column chromatography using 60–120 mesh silica gel with an ethyl acetate and hexane solvent system to afford

**Figure 7**

The reaction scheme for the synthesis of the title compound.

0.3414 g (88% yield) of the title compound (Venugopala *et al.*, 2019). Suitable single crystals of the compound were grown by the slow evaporation of acetone at ambient conditions.

7. Refinement

Crystal data, data collection and structure refinement details are summarized in Table 2. The hydrogen atoms were placed in idealized positions and refined using a riding model with $U_{\text{iso}}(\text{H}) = 1.2U_{\text{eq}}(\text{C})$ or $1.5U_{\text{eq}}(\text{C-methyl})$.

Acknowledgements

The authors are grateful to the Deanship of Scientific Research, King Faisal University, Kingdom of Saudi Arabia for financial support and encouragement. AH thanks IISER Bhopal for a research fellowship. The authors are thankful to the CIF of IISER Bhopal for research facilities and infrastructure.

Funding information

Funding for this research was provided by: Indian Institute of Science Education and Research Bhopal; the Deanship of Scientific Research, King Faisal University, Kingdom of Saudi Arabia (through Research Group grant No. 17122011).

References

- Aslanov, L. A., Tafeenko, V. A., Paseshnichenko, K. A., Bundel', Y. G., Gromov, S. P. & Gerasimov, B. G. (1983). *Zh. Strukt. Khim. (Russ. J. Struct. Chem.)*, **24**, 427–434.
- Barbour, L. J. (2001). *J. Supramol. Chem.* **1**, 189–191.
- Bruker (2008). SAINT and SADABS. Bruker AXS Inc., Madison, Wisconsin, USA.
- Bruker (2012). APEX2. Bruker AXS Inc., Madison, Wisconsin, USA.
- Butler, M. S. (2008). *Nat. Prod. Rep.* **25**, 475–516.
- Chandrashekharappa, S., Venugopala, K. N., Nayak, S. K., Gleiser, R. M., García, D. A., Kumalo, H. M., Kulkarni, R. S., Mahomoodally, F. M., Venugopala, R., Mohan, M. K. & Odhav, B. (2018a). *J. Mol. Struct.* **1156**, 377–384.
- Chandrashekharappa, S., Venugopala, K. N., Tratrat, C., Mahomoodally, F. M., Aldhubiab, B. E., Haroun, M., Venugopala, R., Mohan, M. K., Kulkarni, R. S., Attimarad, M. V., Harsha, S. & Odhav, B. (2018b). *New J. Chem.* **42**, 4893–4901.
- Cingolani, G. M., Claudi, F., Massi, M. & Venturi, F. (1990). *Eur. J. Med. Chem.* **25**, 709–712.
- Dance, I. (2003). *New J. Chem.* **27**, 22–27.
- Gayton, J., Autry, S. A., Meador, W., Parkin, S. R., Hill, G. A. Jr, Hammer, N. I. & Delcamp, J. H. (2019). *J. Org. Chem.* **84**, 687–697.
- Groom, C. R., Bruno, I. J., Lightfoot, M. P. & Ward, S. C. (2016). *Acta Cryst. B72*, 171–179.
- Hathwar, V. R., Bhowal, R. & Chopra, D. (2020). *J. Mol. Struct.* **1208**, 1278642 <https://doi.org/10.1016/j.molstruc.2020.127864>
- Hazra, A., Mondal, S., Maity, A., Naskar, S., Saha, P., Paira, R., Sahu, K. B., Paira, P., Ghosh, S., Sinha, C., Samanta, A., Banerjee, S. & Mondal, N. B. (2011). *Eur. J. Med. Chem.* **46**, 2132–2140.
- Liu, W., Ou, S., He, X., Hu, H., Wu, Q. & Huang, Z. (2003). *J. Chem. Crystallogr.* **33**, 795–798.
- Liu, W.-W., Li, Y.-Z., Sun, R.-K., Hu, H.-W., Wu, Q.-J. & Huang, Z.-X. (2005). *Acta Cryst. E61*, o445–o447.
- Liu, W.-W., Wang, L., Tang, L.-J., Cao, W. & Hu, H.-W. (2007). *Acta Cryst. E63*, o3518.
- Macrae, C. F., Sovago, I., Cottrell, S. J., Galek, P. T. A., McCabe, P., Pidcock, E., Platings, M., Shields, G. P., Stevens, J. S., Towler, M. & Wood, P. A. (2020). *J. Appl. Cryst.* **53**, 226–235.
- McNamara, L. E., Rill, T. A., Huckaba, A. J., Ganeshraj, V., Gayton, J., Nelson, R. A., Sharpe, E. A., Dass, A., Hammer, N. I. & Delcamp, J. H. (2017). *Chem. Eur. J.* **23**, 12494–12501.
- Mederski, W., Beier, N., Burgdorf, L. T., Gericke, R., Klein, M. & Tsaklakidis, C. (2012). US Patent 8(106,067 B2).
- Mishra, B. B. & Tiwari, V. K. (2011). *Opportunity Challenge and Scope of Natural Products in Medicinal Chemistry*, 1–61.
- Qian, B.-H., Liu, W.-W., Lu, L.-D. & Hu, H.-W. (2006). *Acta Cryst. E62*, o2363–o2364.
- Sandeep, C., Padmashali, B., Venugopala, K. N., Kulkarni, R. S., Venugopala, R. & Odhav, B. (2016a). *Asian J. Chem.* **28**, 1043–1048.
- Sandeep, C., Venugopala, K. N., Gleiser, R. M., Chetram, A., Padmashali, B., Kulkarni, R. S., Venugopala, R. & Odhav, B. (2016b). *Chem. Biol. Drug Des.* **88**, 899–904.
- Sheldrick, G. M. (2008). *Acta Cryst. A64*, 112–122.
- Sheldrick, G. M. (2015). *Acta Cryst. C71*, 3–8.
- Sonnenschein, H. & Schneider, M. (1997). *Z. Kristallogr. New Cryst. Struct.* **212**, 161–162.
- Spackman, M. A. & Jayatilaka, D. (2009). *CrystEngComm*, **11**, 19–32.
- Spek, A. L. (2020). *Acta Cryst. E76*, 1–11.
- Tafeenkova, V. A. & Aslanov, L. A. (1980). *Zh. Strukt. Khim.* **21**, 69–78.
- Tafeenkova, V. A. & Au, O. (1996). *Zh. Strukt. Khim.* **37**, 1181–1185.
- Vaught, J. L., Carson, J. R., Carmosin, R. J., Blum, P. S., Persico, F. J., Hageman, W. E., Shank, R. P. & Raffa, R. B. (1990). *J. Pharmacol. Exp. Ther.* **255**, 1–10.
- Venugopala, K. N., Tratrat, C., Pillay, M., Mahomoodally, F. M., Bhandary, S., Chopra, D., Morsy, M. A., Haroun, M., Aldhubiab, B. E., Attimarad, M., Nair, A. B., Sreearsha, N., Venugopala, R., Chandrashekharappa, S., Alwassil, O. I. & Odhav, B. (2019). *Antibiotics*, **8**, 247–263.
- Wolff, S. K., Grimwood, D. J., McKinnon, J. J., Turner, M. J., Jayatilaka, D. & Spackman, M. A. (2012). *CrystalExplorer12.5*. University of Western Australia, Perth.

supporting information

Acta Cryst. (2020). E76, 567-571 [https://doi.org/10.1107/S2056989020003837]

Structural investigation of methyl 3-(4-fluorobenzoyl)-7-methyl-2-phenyl-indolizine-1-carboxylate, an inhibitory drug towards *Mycobacterium tuberculosis*

Avantika Hasija, Subhrajyoti Bhandary, Katharigatta N. Venugopala, Sandeep Chandrashekharappa and Deepak Chopra

Computing details

Data collection: *APEX2* (Bruker, 2012); cell refinement: *SAINT* (Bruker, 2008); data reduction: *SAINT* (Bruker, 2008); program(s) used to solve structure: *SHELXS97* (Sheldrick, 2008); program(s) used to refine structure: *SHELXL2014* (Sheldrick, 2015); molecular graphics: *X-SEED* (Barbour, 2001) and *Mercury* (Macrae *et al.*, 2020); software used to prepare material for publication: *SHELXL2014* (Sheldrick, 2015) and *PLATON* (Spek, 2020).

3-(4-Fluorobenzoyl)-7-methyl-2-phenylindolizine-1-carboxylate

Crystal data

$C_{24}H_{18}FNO_3$
 $M_r = 387.39$
Monoclinic, $P2_1/n$
 $a = 7.3246 (11)$ Å
 $b = 9.8460 (13)$ Å
 $c = 25.837 (4)$ Å
 $\beta = 93.318 (3)^\circ$
 $V = 1860.2 (5)$ Å³
 $Z = 4$

$F(000) = 808$
 $D_x = 1.383 \text{ Mg m}^{-3}$
Mo $K\alpha$ radiation, $\lambda = 0.71073$ Å
Cell parameters from 27523 reflections
 $\theta = 2.2\text{--}27.6^\circ$
 $\mu = 0.10 \text{ mm}^{-1}$
 $T = 173 \text{ K}$
Block, yellow
 $0.32 \times 0.18 \times 0.04$ mm

Data collection

Bruker Kappa Duo APEXII
diffractometer
Radiation source: fine-focus sealed tube
 $0.5^\circ \varphi$ scans and ω scans
Absorption correction: multi-scan
(SADABS; Bruker, 2008)
 $T_{\min} = 0.855$, $T_{\max} = 1.000$
27523 measured reflections

4296 independent reflections
2641 reflections with $I > 2\sigma(I)$
 $R_{\text{int}} = 0.090$
 $\theta_{\max} = 27.6^\circ$, $\theta_{\min} = 2.2^\circ$
 $h = -9 \rightarrow 9$
 $k = -12 \rightarrow 12$
 $l = -33 \rightarrow 33$

Refinement

Refinement on F^2
Least-squares matrix: full
 $R[F^2 > 2\sigma(F^2)] = 0.050$
 $wR(F^2) = 0.131$
 $S = 1.00$
4296 reflections
265 parameters

0 restraints
Primary atom site location: structure-invariant direct methods
Secondary atom site location: difference Fourier map
Hydrogen site location: inferred from neighbouring sites

H-atom parameters constrained
 $w = 1/[\sigma^2(F_o^2) + (0.0555P)^2 + 0.455P]$
 where $P = (F_o^2 + 2F_c^2)/3$
 $(\Delta/\sigma)_{\text{max}} < 0.001$
 $\Delta\rho_{\text{max}} = 0.29 \text{ e } \text{\AA}^{-3}$

$\Delta\rho_{\text{min}} = -0.30 \text{ e } \text{\AA}^{-3}$
 Extinction correction: SHELXL-2014/7
 (Sheldrick 2015,
 $F_c^* = kFc[1+0.001xFc^2\lambda^3/\sin(2\theta)]^{-1/4}$
 Extinction coefficient: 0.0044 (8)

Special details

Geometry. All esds (except the esd in the dihedral angle between two l.s. planes) are estimated using the full covariance matrix. The cell esds are taken into account individually in the estimation of esds in distances, angles and torsion angles; correlations between esds in cell parameters are only used when they are defined by crystal symmetry. An approximate (isotropic) treatment of cell esds is used for estimating esds involving l.s. planes.

Fractional atomic coordinates and isotropic or equivalent isotropic displacement parameters (\AA^2)

	<i>x</i>	<i>y</i>	<i>z</i>	$U_{\text{iso}}^*/U_{\text{eq}}$
F1	0.4480 (2)	0.70181 (14)	0.32107 (5)	0.0563 (4)
O1	0.2787 (2)	0.69998 (15)	0.00174 (6)	0.0381 (4)
O2	0.1668 (2)	0.53237 (14)	-0.04937 (5)	0.0302 (4)
O3	0.5350 (2)	0.21447 (15)	0.16777 (5)	0.0336 (4)
N1	0.3494 (2)	0.26669 (16)	0.06884 (6)	0.0230 (4)
C1	0.3588 (3)	0.1276 (2)	0.07210 (8)	0.0293 (5)
H1	0.4025	0.0857	0.1035	0.035*
C2	0.3057 (3)	0.0502 (2)	0.03060 (8)	0.0294 (5)
H2	0.3148	-0.0459	0.0330	0.035*
C3	0.2368 (3)	0.1106 (2)	-0.01642 (8)	0.0269 (5)
C4	0.2282 (3)	0.2488 (2)	-0.01917 (7)	0.0252 (5)
H4	0.1830	0.2906	-0.0505	0.030*
C5	0.2850 (3)	0.3307 (2)	0.02346 (7)	0.0232 (4)
C6	0.2913 (3)	0.4722 (2)	0.03281 (7)	0.0232 (4)
C7	0.3565 (3)	0.4924 (2)	0.08437 (7)	0.0225 (4)
C8	0.3910 (3)	0.3647 (2)	0.10738 (7)	0.0229 (4)
C9	0.1754 (3)	0.0225 (2)	-0.06142 (8)	0.0356 (5)
H9A	0.1001	0.0760	-0.0865	0.053*
H9B	0.1035	-0.0537	-0.0491	0.053*
H9C	0.2826	-0.0125	-0.0781	0.053*
C10	0.2478 (3)	0.5806 (2)	-0.00470 (7)	0.0248 (5)
C11	0.1182 (3)	0.6340 (2)	-0.08794 (8)	0.0315 (5)
H11A	0.0323	0.6988	-0.0739	0.047*
H11B	0.0606	0.5902	-0.1188	0.047*
H11C	0.2285	0.6822	-0.0974	0.047*
C12	0.3881 (3)	0.6250 (2)	0.11063 (7)	0.0250 (5)
C13	0.5610 (3)	0.6581 (2)	0.13180 (7)	0.0287 (5)
H13	0.6610	0.5989	0.1269	0.034*
C14	0.5889 (3)	0.7767 (2)	0.15993 (8)	0.0363 (6)
H14	0.7076	0.7984	0.1743	0.044*
C15	0.4445 (4)	0.8634 (2)	0.16707 (8)	0.0387 (6)
H15	0.4631	0.9443	0.1867	0.046*
C16	0.2724 (4)	0.8320 (2)	0.14543 (8)	0.0390 (6)
H16	0.1729	0.8918	0.1502	0.047*

C17	0.2443 (3)	0.7144 (2)	0.11693 (8)	0.0326 (5)
H17	0.1263	0.6945	0.1016	0.039*
C18	0.4633 (3)	0.3265 (2)	0.15900 (7)	0.0253 (5)
C19	0.4534 (3)	0.4247 (2)	0.20269 (7)	0.0257 (5)
C20	0.6087 (3)	0.4441 (2)	0.23563 (8)	0.0324 (5)
H20	0.7157	0.3924	0.2307	0.039*
C21	0.6082 (3)	0.5381 (2)	0.27542 (8)	0.0385 (6)
H21	0.7144	0.5534	0.2975	0.046*
C22	0.4491 (4)	0.6086 (2)	0.28191 (8)	0.0374 (6)
C23	0.2923 (3)	0.5899 (2)	0.25163 (8)	0.0328 (5)
H23	0.1843	0.6393	0.2579	0.039*
C24	0.2955 (3)	0.4967 (2)	0.21143 (8)	0.0283 (5)
H24	0.1883	0.4820	0.1897	0.034*

Atomic displacement parameters (\AA^2)

	U^{11}	U^{22}	U^{33}	U^{12}	U^{13}	U^{23}
F1	0.0812 (12)	0.0445 (9)	0.0415 (8)	0.0051 (8)	-0.0116 (7)	-0.0201 (7)
O1	0.0596 (11)	0.0203 (8)	0.0333 (8)	-0.0034 (7)	-0.0062 (7)	0.0057 (7)
O2	0.0413 (9)	0.0238 (8)	0.0248 (7)	0.0018 (7)	-0.0048 (6)	0.0033 (6)
O3	0.0420 (9)	0.0259 (8)	0.0323 (8)	0.0073 (7)	-0.0035 (7)	0.0032 (7)
N1	0.0271 (10)	0.0201 (9)	0.0219 (8)	0.0005 (7)	0.0025 (7)	0.0018 (7)
C1	0.0363 (13)	0.0213 (11)	0.0304 (11)	0.0029 (9)	0.0019 (9)	0.0052 (9)
C2	0.0369 (13)	0.0192 (11)	0.0324 (11)	0.0007 (9)	0.0036 (9)	-0.0004 (9)
C3	0.0282 (11)	0.0251 (12)	0.0280 (11)	-0.0045 (9)	0.0057 (9)	-0.0019 (9)
C4	0.0282 (11)	0.0248 (11)	0.0228 (10)	-0.0010 (9)	0.0020 (8)	0.0008 (8)
C5	0.0235 (10)	0.0234 (11)	0.0228 (10)	0.0005 (8)	0.0032 (8)	0.0033 (8)
C6	0.0255 (11)	0.0214 (10)	0.0228 (10)	0.0001 (8)	0.0020 (8)	0.0010 (8)
C7	0.0239 (11)	0.0206 (10)	0.0233 (10)	0.0014 (8)	0.0028 (8)	0.0005 (8)
C8	0.0260 (11)	0.0207 (10)	0.0219 (9)	0.0001 (8)	0.0021 (8)	-0.0014 (8)
C9	0.0460 (14)	0.0281 (12)	0.0326 (12)	-0.0038 (10)	0.0005 (10)	-0.0039 (10)
C10	0.0268 (11)	0.0243 (11)	0.0237 (10)	0.0000 (9)	0.0033 (8)	0.0015 (9)
C11	0.0382 (13)	0.0302 (12)	0.0256 (10)	0.0028 (10)	-0.0036 (9)	0.0077 (9)
C12	0.0373 (12)	0.0183 (10)	0.0197 (9)	-0.0001 (9)	0.0028 (9)	0.0029 (8)
C13	0.0375 (12)	0.0237 (11)	0.0253 (10)	-0.0035 (9)	0.0056 (9)	0.0008 (9)
C14	0.0494 (15)	0.0283 (12)	0.0311 (12)	-0.0106 (11)	0.0033 (11)	-0.0014 (10)
C15	0.0653 (17)	0.0199 (12)	0.0311 (12)	-0.0025 (11)	0.0026 (11)	-0.0030 (10)
C16	0.0589 (16)	0.0251 (12)	0.0333 (12)	0.0136 (11)	0.0062 (11)	0.0012 (10)
C17	0.0407 (13)	0.0267 (12)	0.0301 (11)	0.0059 (10)	-0.0009 (10)	0.0018 (9)
C18	0.0254 (11)	0.0259 (11)	0.0247 (10)	-0.0020 (9)	0.0026 (8)	0.0024 (9)
C19	0.0344 (12)	0.0223 (11)	0.0202 (9)	-0.0025 (9)	0.0000 (9)	0.0045 (8)
C20	0.0371 (13)	0.0289 (12)	0.0305 (11)	0.0013 (10)	-0.0046 (10)	0.0022 (10)
C21	0.0498 (16)	0.0324 (13)	0.0316 (12)	-0.0036 (11)	-0.0130 (11)	0.0016 (10)
C22	0.0614 (17)	0.0235 (12)	0.0268 (11)	-0.0004 (11)	-0.0024 (11)	-0.0027 (9)
C23	0.0420 (14)	0.0298 (12)	0.0269 (11)	0.0020 (10)	0.0058 (10)	0.0018 (9)
C24	0.0346 (12)	0.0274 (12)	0.0228 (10)	-0.0028 (9)	0.0010 (9)	0.0018 (9)

Geometric parameters (\AA , $\text{^{\circ}}$)

F1—C22	1.367 (2)	C11—H11A	0.9800
O1—C10	1.206 (2)	C11—H11B	0.9800
O2—C10	1.353 (2)	C11—H11C	0.9800
O2—C11	1.442 (2)	C12—C13	1.389 (3)
O3—C18	1.236 (2)	C12—C17	1.389 (3)
N1—C1	1.373 (3)	C13—C14	1.384 (3)
N1—C5	1.389 (2)	C13—H13	0.9500
N1—C8	1.408 (2)	C14—C15	1.380 (3)
C1—C2	1.354 (3)	C14—H14	0.9500
C1—H1	0.9500	C15—C16	1.384 (3)
C2—C3	1.419 (3)	C15—H15	0.9500
C2—H2	0.9500	C16—C17	1.382 (3)
C3—C4	1.364 (3)	C16—H16	0.9500
C3—C9	1.499 (3)	C17—H17	0.9500
C4—C5	1.409 (3)	C18—C19	1.491 (3)
C4—H4	0.9500	C19—C24	1.387 (3)
C5—C6	1.414 (3)	C19—C20	1.393 (3)
C6—C7	1.403 (3)	C20—C21	1.383 (3)
C6—C10	1.465 (3)	C20—H20	0.9500
C7—C8	1.407 (3)	C21—C22	1.375 (3)
C7—C12	1.483 (3)	C21—H21	0.9500
C8—C18	1.456 (3)	C22—C23	1.364 (3)
C9—H9A	0.9800	C23—C24	1.388 (3)
C9—H9B	0.9800	C23—H23	0.9500
C9—H9C	0.9800	C24—H24	0.9500
C10—O2—C11	115.09 (16)	H11A—C11—H11C	109.5
C1—N1—C5	121.17 (17)	H11B—C11—H11C	109.5
C1—N1—C8	129.22 (17)	C13—C12—C17	119.06 (19)
C5—N1—C8	109.56 (16)	C13—C12—C7	120.09 (18)
C2—C1—N1	120.09 (19)	C17—C12—C7	120.76 (19)
C2—C1—H1	120.0	C14—C13—C12	120.5 (2)
N1—C1—H1	120.0	C14—C13—H13	119.7
C1—C2—C3	120.92 (19)	C12—C13—H13	119.7
C1—C2—H2	119.5	C15—C14—C13	120.1 (2)
C3—C2—H2	119.5	C15—C14—H14	120.0
C4—C3—C2	118.41 (18)	C13—C14—H14	120.0
C4—C3—C9	121.74 (19)	C14—C15—C16	119.7 (2)
C2—C3—C9	119.85 (18)	C14—C15—H15	120.2
C3—C4—C5	121.33 (19)	C16—C15—H15	120.2
C3—C4—H4	119.3	C17—C16—C15	120.4 (2)
C5—C4—H4	119.3	C17—C16—H16	119.8
N1—C5—C4	118.07 (18)	C15—C16—H16	119.8
N1—C5—C6	107.26 (16)	C16—C17—C12	120.2 (2)
C4—C5—C6	134.66 (18)	C16—C17—H17	119.9
C7—C6—C5	107.94 (17)	C12—C17—H17	119.9

C7—C6—C10	125.01 (18)	O3—C18—C8	121.78 (18)
C5—C6—C10	126.97 (17)	O3—C18—C19	118.57 (17)
C6—C7—C8	108.49 (17)	C8—C18—C19	119.64 (17)
C6—C7—C12	126.51 (17)	C24—C19—C20	119.31 (19)
C8—C7—C12	124.99 (17)	C24—C19—C18	122.16 (18)
C7—C8—N1	106.72 (16)	C20—C19—C18	118.54 (19)
C7—C8—C18	131.69 (18)	C21—C20—C19	120.6 (2)
N1—C8—C18	121.52 (17)	C21—C20—H20	119.7
C3—C9—H9A	109.5	C19—C20—H20	119.7
C3—C9—H9B	109.5	C22—C21—C20	117.8 (2)
H9A—C9—H9B	109.5	C22—C21—H21	121.1
C3—C9—H9C	109.5	C20—C21—H21	121.1
H9A—C9—H9C	109.5	C23—C22—F1	118.3 (2)
H9B—C9—H9C	109.5	C23—C22—C21	123.6 (2)
O1—C10—O2	121.96 (18)	F1—C22—C21	118.1 (2)
O1—C10—C6	125.95 (18)	C22—C23—C24	117.9 (2)
O2—C10—C6	112.09 (17)	C22—C23—H23	121.0
O2—C11—H11A	109.5	C24—C23—H23	121.0
O2—C11—H11B	109.5	C19—C24—C23	120.7 (2)
H11A—C11—H11B	109.5	C19—C24—H24	119.6
O2—C11—H11C	109.5	C23—C24—H24	119.6
C5—N1—C1—C2	0.4 (3)	C7—C6—C10—O2	-172.44 (18)
C8—N1—C1—C2	177.53 (19)	C5—C6—C10—O2	11.1 (3)
N1—C1—C2—C3	-1.2 (3)	C6—C7—C12—C13	-121.3 (2)
C1—C2—C3—C4	1.2 (3)	C8—C7—C12—C13	57.4 (3)
C1—C2—C3—C9	-178.8 (2)	C6—C7—C12—C17	62.2 (3)
C2—C3—C4—C5	-0.4 (3)	C8—C7—C12—C17	-119.0 (2)
C9—C3—C4—C5	179.56 (19)	C17—C12—C13—C14	1.7 (3)
C1—N1—C5—C4	0.4 (3)	C7—C12—C13—C14	-174.86 (18)
C8—N1—C5—C4	-177.26 (17)	C12—C13—C14—C15	-0.2 (3)
C1—N1—C5—C6	179.55 (18)	C13—C14—C15—C16	-0.8 (3)
C8—N1—C5—C6	1.9 (2)	C14—C15—C16—C17	0.2 (3)
C3—C4—C5—N1	-0.4 (3)	C15—C16—C17—C12	1.3 (3)
C3—C4—C5—C6	-179.2 (2)	C13—C12—C17—C16	-2.2 (3)
N1—C5—C6—C7	-1.1 (2)	C7—C12—C17—C16	174.28 (19)
C4—C5—C6—C7	177.8 (2)	C7—C8—C18—O3	-157.8 (2)
N1—C5—C6—C10	175.82 (18)	N1—C8—C18—O3	19.0 (3)
C4—C5—C6—C10	-5.3 (4)	C7—C8—C18—C19	21.5 (3)
C5—C6—C7—C8	0.0 (2)	N1—C8—C18—C19	-161.76 (18)
C10—C6—C7—C8	-177.05 (19)	O3—C18—C19—C24	-134.5 (2)
C5—C6—C7—C12	178.88 (19)	C8—C18—C19—C24	46.2 (3)
C10—C6—C7—C12	1.9 (3)	O3—C18—C19—C20	45.5 (3)
C6—C7—C8—N1	1.2 (2)	C8—C18—C19—C20	-133.8 (2)
C12—C7—C8—N1	-177.78 (18)	C24—C19—C20—C21	-2.6 (3)
C6—C7—C8—C18	178.3 (2)	C18—C19—C20—C21	177.43 (19)
C12—C7—C8—C18	-0.7 (3)	C19—C20—C21—C22	1.4 (3)
C1—N1—C8—C7	-179.3 (2)	C20—C21—C22—C23	0.6 (3)

C5—N1—C8—C7	−1.9 (2)	C20—C21—C22—F1	−179.8 (2)
C1—N1—C8—C18	3.2 (3)	F1—C22—C23—C24	178.97 (19)
C5—N1—C8—C18	−179.35 (17)	C21—C22—C23—C24	−1.4 (3)
C11—O2—C10—O1	−1.0 (3)	C20—C19—C24—C23	1.7 (3)
C11—O2—C10—C6	179.33 (17)	C18—C19—C24—C23	−178.30 (19)
C7—C6—C10—O1	7.9 (3)	C22—C23—C24—C19	0.2 (3)
C5—C6—C10—O1	−168.6 (2)		

Hydrogen-bond geometry (Å, °)

D—H···A	D—H	H···A	D···A	D—H···A
C1—H1···O3	0.95	2.26	2.853 (3)	120
C4—H4···O2	0.95	2.38	2.927 (2)	116
C21—H21···O3 ⁱ	0.95	2.54	3.399 (3)	149
C2—H2···O1 ⁱⁱ	0.95	2.63	3.531 (4)	157
C15—H15···O3 ⁱⁱⁱ	0.95	2.76	3.519 (4)	137
C1—H1···C15 ⁱⁱ	0.95	2.74	3.6064 (3)	152
C11—H11A···C5 ^{iv}	0.98	2.74	3.4906 (1)	133
C11—H11B···F1 ^v	0.98	2.67	3.0585 (3)	104
C23—H23···O3 ^{vi}	0.95	2.67	3.4875 (3)	143

Symmetry codes: (i) $-x+3/2, y+1/2, -z+1/2$; (ii) $x, y-1, z$; (iii) $x, y+1, z$; (iv) $-x, -y+1, -z$; (v) $x-1/2, -y+3/2, z-1/2$; (vi) $-x+1/2, y+1/2, -z+1/2$.